LUND UNIVERSITY

Effects of peptide hydrophobicity on its incorporation in phospholipid membranes - an NMR and ellipsometry study

Oradd, Greger; Schmidtchen, Artur; Malmsten, Martin

Link to publication

LUP

Lund University Publications

Institutional Repository of Lund University

Effects of peptide hydrophobicity on its incorporation in phospholipid membranes – an NMR and ellipsometry study

Greger Orädd[1], Artur Schmidtchen[2], and Martin Malmsten[3,*]

[1]Department of Biophysical Chemistry, Umeå University, SE-90187, Umeå, Sweden
[2]Divison of Dermatology and Venereology, Department of Clinical Sciences, Lund University, SE-221 84 Lund, Sweden
[3]Department of Pharmacy, Uppsala University, SE-75123, Uppsala, Sweden.

[*]Corresponding author. Tel: +46184714334; Fax: +46184714377; E-mail: martin.malmsten@farmaci.uu.se

Abstract

Effects of peptide hydrophobicity on lipid membrane binding, incorporation, and defect formation was investigated for variants of the complement-derived antimicrobial peptide CNY21 (CNYITELRRQHARASHLGLAR), in anionic 1-palmitoyl-2-oleoylphosphatidylethanolamine (POPE)/1-palmitoyl-2-oleoylphosphatidylglycerol (POPG) and zwitterionic 1-palmitoyl-2-oleoylphosphatidylcholine (POPC) membranes. Using a method combination of, e.g., ellipsometry, CD, and fluorescence spectroscopy, it was shown that peptide adsorption, as well as peptide-induced liposome leakage and bactericidal potency against *Escherichia coli* and *Pseudomonas aeruginosa*, was promoted by increasing the hydrophobicity of CNY21 through either substituting the two histidines (H) in CNY21 with more hydrophobic leucine (L) residues, or end-tagging with tritryptophan (WWW). Fluorescence spectroscopy revealed that both CNY21WWW and the WWW tripeptide localized to the polar headgroup region of these phospholipid membranes. Deuterium NMR experiments on macroscopically oriented membranes containing fully (palmitoyl) deuterated POPC (POPC-d_{31}) demonstrated that both CNY21L and CNY21WWW induced disordering of the lipid membrane. In contrast, for cholesterol-supplemented POPC-d_{31} bilayers, peptide-induced disordering was less pronounced in the case of CNY21L, indicating that the peptide is unable to partition to the interior of the lipid membrane in the presence of cholesterol. CNY21WWW, on the other hand, retained its membrane-disordering effect also for cholesterol-supplemented POPC-d_{31}. These findings were supported by pulsed field gradient NMR experiments where the lateral lipid diffusion was determined in the absence and presence of peptides. Overall, the results provide some mechanistic understanding to previously observed effects of peptide hydrophobization through point mutations and end-tagging, particularly so for complement-based antimicrobial peptides.

Introduction

As a result of increasing occurrence of multidrug-resistant bacteria, antimicrobial peptides (AMPs), are currently receiving increased attention (1-8). Through use of, e.g., quantitative structure-activity relationship investigations (QSAR) in combination with directed amino acid modifications (9-11), or identification of AMPs of endogenous origin (12-14), high bactericidal potency can be reached also at low toxicity against (human) eukaryotic cells. Although AMPs influence bacteria in a number of ways, bacterial membrane rupture is a key mechanism of action of these peptides (2-5,15-18), Since bacterial membranes are cholesterol-void and dominated by anionic phospholipids, whereas (human) eukaryotic membranes contain cholesterol and are dominated by zwitterionic ones, some AMP selectivity can be obtained for positively charged and hydrophilic AMPs. However, *Staphylococcus aureus* and a number of other common pathogens typically display a limited electrostatic surface potential, which may be reduced or even reversed in various ways (6). Furthermore, the membrane binding of such peptides is salt sensitive, and their bactericidal potency at physiological ionic strength limited. This shortcoming can be addressed by increasing the hydrophobicity of AMPs, although highly hydrophobic AMPs have been found to be less selective in their action, thus displaying increased toxicity (4). Given the above, we previously identified modest hydrophobic modification of complement-based AMPs (15), as well as hydrophobic end-tagging of AMPs with hydrophobic amino acid stretches (19-22), as a way to promote peptide binding and membrane disruption, and to reduce salt sensitivity of AMPs. Particularly the end-tagged peptides were demonstrated to display limited toxicity combined with high microbicidal potency of broad spectrum, also at physiological ionic strength and in the presence of serum, as well as *ex vivo* and *in vivo*. While it could be demonstrated that the increased potency of these peptides was due to the hydrophobic modification promoting peptide adsorption at phospholipid membranes, the finer details of the effect of the hydrophobic modifications remained to be elucidated.

Given this, the present study aims to bring this work further by investigating the effects of hydrophobic modifications on peptide incorporation into phospholipid membranes. In doing so, we employ a method combination of liposome leakage assay, ellipsometry, as well as CD and fluorescence spectroscopy, and combine this with NMR spectroscopy techniques for macroscopically oriented membranes, aimed at elucidating effects of peptide incorporate into

the membranes on the ordering and diffusion of lipid molecules. Furthermore, two different types of hydrophobic modifications are compared for the complement-derived peptide CNY21, i.e., single amino acid substitutions within the template peptide sequence, and hydrophobic end-tagging (Table 1). In addition, effects of cholesterol were investigated.

Experimental

Peptides. Peptides were synthesized by Biopeptide Co., San Diego, USA. The purity (>95%) of these peptides was confirmed by mass spectral analysis (MALDI-ToF Voyager). Prior to experiments, peptides were diluted in H_2O (5 mM stock), and stored at –20 C. This stock solution was used for the subsequent experiments.

Microorganisms. *Escherichia coli* ATCC 25922 and *Pseudomonas aeruginosa* clinical isolate 27.1 were obtained from the Department of Clinical Bacteriology at Lund University Hospital, Sweden.

Viable count analysis. *E. coli* ATCC 25922 or *P. aeruginosa* 27.1 were grown overnight in full-strength (3% w/v) trypticase soy broth (TSB) (Becton-Dickinson, Cockeysville, USA) and washed twice with 10 mM Tris, pH 7.4, before diluting in 10 mM Tris, pH 7.4, containing 5 mM glucose. Following this, bacteria (50 µl; $1\text{-}2\times10^6$ CFU/mL) were incubated at 37°C for 2 hours at a range of concentrations (0, 10, 30 µM) with peptides in 10 mM Tris, pH 7.4, containing 5 mM glucose in presence of 0.15 M NaCl. Serial dilutions of the incubated mixtures were plated on TH agar, followed by incubation at 37°C overnight, and determination of the number of colony-forming units. Results are given as survival after exposure to peptide, where 100% survival was defined as total survival of bacteria in the same buffer and under the same condition in the absence of peptide.

Liposome preparation and leakage assay. The liposomes investigated were either zwitterionic (POPC-d_{31}/cholesterol 60/40 mol/mol or POPC-d_{31} without cholesterol) or anionic (POPE/POPG 75/25 mol/mol). POPG (1-palmitoyl-2-oleoyl-*sn*-Glycero-3-phosphoglycerol, monosodium salt), POPE (1-palmitoyl-2-oleoyl-*sn*-Glycero-3-phoshoetanolamine), and POPC-d_{31} (fully (palmitoyl) deuterated 1-palmitoyl-2-oleoyl-*sn*-glycero-3-phoshocholine) were all from Avanti Polar Lipids (Alabaster, USA) and of >99%

purity, while cholesterol (>99% purity), was from Sigma-Aldrich (St. Louis, USA). These lipid systems were chosen primarily for methodological reasons, as they offer good membrane cohesion, thus facilitating stable unilamellar liposomes and well defined supported lipid bilayers, allowing detailed values on leakage and adsorption density to be obtained. In addition, POPC is available in deuterated form, a reqirement for the NMR experiments employed. The lipid mixtures were dissolved in chloroform, after which solvent was removed by evaporation under vacuum overnight. Subsequently, 10 mM Tris buffer, pH 7.4, was added together with 0.1 M carboxyfluorescein (CF) (Sigma, St. Louis, USA). After hydration, the lipid mixture was subjected to eight freeze-thaw cycles consisting of freezing in liquid nitrogen and heating to 60°C. Unilamellar liposomes of about Ø140 nm were generated by multiple extrusions through polycarbonate filters (pore size 100 nm) mounted in a LipoFast miniextruder (Avestin, Ottawa, Canada) at 22°C. Untrapped CF was removed by two subsequent gel filtrations (Sephadex G-50, GE Healthcare, Uppsala, Sweden) at 22°C, with Tris buffer as eluent. CF release from the liposomes was determined by monitoring the emitted fluorescence at 520 nm from a liposome dispersion (10 µM lipid in 10 mM Tris, pH 7.4). An absolute leakage scale was obtained by disrupting the liposomes at the end of each experiment through addition of 0.8 mM Triton X-100 (Sigma-Aldrich, St. Louis, USA). A SPEX-fluorolog 1650 0.22-m double spectrometer (SPEX Industries, Edison, USA) was used for the liposome leakage assay. Measurements were performed in triplicate at 37 °C.

Fluorescence spectroscopy. Tryptophan fluorescence spectra were determined by a SPEX Fluorolog-2 spectrofluorometer at a peptide concentration of 10 µM. An excitation wavelength of 280 nm was used, while emission spectra were taken between 300 and 450 nm. Measurements were conducted at 37°C while stirring in either 10 mM Tris, pH 7.4. Where indicated, liposomes (100 µM lipid) were included, incubated with the peptides for one hour before measurements were initiated.

CD spectroscopy. Circular dichroism (CD) spectra were measured by a Jasco J-810 Spectropolarimeter (Jasco, Easton, USA). The measurements were performed in duplicate at 37°C in a 10 mm quartz cuvette under stirring with a peptide concentration of 10 µM. The effect on peptide secondary structure of liposomes at a lipid concentration of 100 µM was monitored in the range 200-260 nm. To account for instrumental differences between

measurements, the background value (detected at 250 nm, where no peptide signal is present) was subtracted. Signals from the bulk solution were also corrected for.

Ellipsometry. Peptide adsorption to supported lipid bilayers was studied *in situ* by null ellipsometry, using an Optrel Multiskop (Optrel, Kleinmachnow, Germany) equipped with a 100 mW argon laser. All measurements were carried out at 532 nm and an angle of incidence of 67.66° in a 5 ml cuvette under stirring (300 rpm). Both the principles of null ellipsometry and the procedures used have been described extensively before (23,24). In brief, by monitoring the change in the state of polarization of light reflected at a surface in the absence and presence of an adsorbed layer, the mean refractive index (n) and layer thickness (d) of the adsorbed layer can be obtained. From the thickness and refractive index the adsorbed amount (Γ) was calculated according to (25):

$$\Gamma = \frac{(n - n_0)}{dn/dc} d \qquad\qquad (1)$$

where dn/dc is the refractive index increment (0.154 cm^3/g) and n_0 is the refractive index of the bulk solution. Corrections were routinely done for changes in bulk refractive index caused by changes in temperature and excess electrolyte concentration.

Phospholipid bilayers were deposited on silica surfaces (electric surface potential -40 mV and contact angle of <10° (26)) by co-adsorption from a mixed micellar solution containing 60/40 mol/mol POPC-d$_{31}$/cholesterol and n-dodecyl-β-D-maltoside (DDM; ≥98% purity, Sigma-Aldrich, St. Louis, USA), as described in detail previously for dioleoyldiphosphatidylcholine (24). In brief, the mixed micellar solution was formed by addition of 19 mM DDM in water to POPC-d$_{31}$/cholesterol dry lipid films, followed by stirring over night, yielding a solution containing 97.3 mol% DDM, 1.6 mol% POPC-d$_{31}$ and 1.1 mol% cholesterol. This micellar solution was added to the cuvette at 25°C, and the following adsorption monitored as a function of time. When adsorption had stabilised, rinsing with Milli-Q water at 5 ml/min was initiated to remove mixed micelles from solution and surfactant from the substrate. By repeating this procedure and subsequently lowering the concentration of the micellar solution, stable and densely packed bilayers are formed, with structural characteristics similar to those of bulk lamellar structures of the lipids (16,24).

After lipid bilayer formation, temperature was raised and the cuvette content replaced by buffer at a rate of 5 ml/min over a period of 30 minutes. After stabilization for 40 minutes, peptide was added to a concentration of 0.01 µM, followed by three subsequent peptide additions to 0.1 µM, 0.5 mM and 1 mM, in all cases monitoring the adsorption for one hour. All measurements were made in at least duplicate.

Preparation of macroscopically oriented bilayers

Fully hydrated samples consisting of POPC-d_{31} (±cholesterol) with the addition of the various peptides were prepared and oriented between glass plates according to previously published methods (27). Briefly, lipid, peptide, and buffer salts were dissolved in MeOH/CHCl$_3$ (3:2 vol/vol), placed on glass plates, and solvent removed by evaporation. The glass plates were stacked in a sample holder and subsequently placed in a humid atmosphere for one week, during which hydrated bilayers were formed, with an orientation along the glass plates. While water content could not be checked for the samples, it is estimated to be close to the maximum hydration of the lipids, i.e., between 30-40% wt, based on hydration kinetics of other samples of similar composition (28), thus yielding a buffer concentration of 12-17 mM. Peptide/lipid weight ratios used were 5/95 for CNY21WWW and CNY21L, and 1.36/98.64 for WWW.

NMR measurements

NMR measurements were performed on a Chemagnetics Infinity NMR spectrometer (Varian, Fort Collins, USA) equipped with a goniometer probe allowing the macroscopically aligned bilayers to be oriented with the bilayer normal at the desired angle with respect to the main magnetic field, and capable of producing magnetic field gradients up to 10 T/m. The temperature was held at 37 ± 0.5ºC by means of a heated air stream passing the sample. The ^{2}H measurements were performed at a frequency of 61.48 MHz. Spectra were recorded with the quadrupole spin-echo sequence using composite pulses (29) to ensure complete spectral coverage and the 0 degree orientation set by maximizing the observed quadrupole splittings (c.f., Eq. (2)). The hard 90° pulse length was measured to 11 ms, which gives a uniform excitation profile up to ±57 kHz for the composite pulses. Each C-^{2}H$_2$ segment of the lipid chain gives rise to a Pake doublet, i.e., two lines at frequencies ±ν. The frequency separation of the peaks, so called residual quadrupole splitting ($\Delta\nu_q$), is given by:

$$\Delta\nu_q = \nu_q S_{CD}(3\cos^2\theta_{LD} - 1) \qquad\qquad (2)$$

in which the quadrupole coupling constant ν_q takes the value 127.5 kHz for a C-^{2}H-bond (30). S_{CD} is the order parameter of the C-^{2}H bond and θ_{LD} is the angle between the bilayer normal and the main magnetic field (31). The resulting spectra are shown in Figure 5. Due to differences in the order parameters among the C-^{2}H$_2$ segments, spectra of well oriented samples consist of several Pake doublets corresponding to different residual quadrupole splittings, where the innermost doublet corresponds to the terminal methyl group of the chain. $\Delta\nu_q$ was considerably smaller for this group due to the additional averaging caused by the free rotation around the C-C bond.

The lipid lateral diffusion was measured according to well established methods (27,32) with the stimulated spin-echo method (33) with the LED modification (34) to eliminate artefacts arising from eddy currents. In order to remove static dipolar couplings, which would prevent the spin-echo to form, samples were oriented with the bilayer normal at 54.7º with respect to the main magnetic field (27,32). The intensity of the signal from a molecule experiencing free Brownian diffusion is given by (33):

$$A = A_0\exp(-\gamma^2\delta^2 g^2 D(\Delta-\delta/3)) \qquad\qquad (3)$$

where A_0 is a factor proportional to the proton content in the system, γ is the gyromagnetic ratio, Δ is the time interval between two identical gradient pulses, $(\Delta-\delta/3)$ is the diffusion time, δ and g are the duration and amplitude of the pulsed field gradients, respectively, and D is the self-diffusion coefficient. Several measurements were made for each sample, in which all parameters except g were kept constant, while g was varied in twenty steps between 0.60-9.52 T/m. δ was 3 ms, and Δ was either 15 or 100 ms. The resulting spectra consists of overlapping spectra from the different diffusion components and the diffusion coefficients were determined by use of the CORE method (35). Finally, since the pulsed field gradient was directed along the main magnetic field, the lateral (in-plane) diffusion coefficient D_L was calculated from its projection as 1.5·D (27).

The analysis resulted in one diffusion component in the range of 300-500 μm^2/s, which was assigned to water and was not analyzed further. The second spectra component originated

from the lipid and the results are reported in Figure 7. The error bars shown in this figure are based on the variation in the results for repeated measurements on the same sample as well as from duplicate samples.

Results and discussion

As a first step, effects of increasing peptide hydrophobicity on peptide-induced liposome leakage was investigated. As shown in Figure 1a, native CNY21 displayed modest leakage induction for POPC-d_{31} liposomes, comparable to that found previously for dioleoylphosphatidylcholine (DOPC) liposomes (18). Increasing peptide hydrophobicity through H->L modifications (CNY21L) or through end-tagging with WWW (CNY21WWW) resulted in a drastically increased liposome leakage, again in agreement with previous observations for DOPC liposomes (18,19). In comparison, the WWW tripeptide caused only modest liposome leakage induction. For cholesterol-supplemented liposomes (POPC-d_{31}/cholesterol 60/40 mol/mol), similar results were observed, although peptide-induced leakage induction throughout was quantitatively somewhat lower for the cholesterol-supplemented liposomes, as expected from the well-known membrane-stabilizing effect of cholesterol (36) (Figure 1b). Similar effects of peptide hydrophobicity was observed also for anionic POPE/POPG (75/25 mol/mol) liposomes (Supporting Material, Figure S1). Thus, both H->L modification and WWW-tagging caused increased peptide-induced liposome leakage, while the WWW tripeptide was largely inefficient in causing liposome rupture. Taken together, the above results clearly domonstrate the importance of hydrophobic interaction for the membrane-disruptive capacity of CNY21. This is not to say that electrostatic interactions do not play a role in the membrae action of the positively charged CNY21. Thus, as demonstrated previously (15), anionic DOPA-based membranes (z-potential $\approx$ -32mV) adsorbs CNY21 and related peptides roughly three-fold more than zwitterionic DOPC-based membranes (z-potential $\approx$-10 mV). Furthermore, removing the charges of CNY21 through R->S substitutions resulted in complete elimination of both peptide adsorption to membranes and resulting membrane disruption and antibacterial effect.

Similarly, while not being of primary interest to the present investigation and also demonstrating some spread between bacterial strains, CNY21L and CNY21WWW displayed increased bactericidal potency, compared to that of the native CNY21 peptide, while the

WWW tripeptide displayed very modest bactericidal effect (Supporting Material, Figure S2). Thus, while bacteria lipid membranes are obviously very different from d_{31}-POPC liposomes, not only from a lipid composition perspective (headgroup as well as acyl group composition), but also from neglecting the abundance of protein and other non-lipid components present in bacterial membranes (37-40), results obtained for POPC-d_{31} bear at least some relevance also to bacterial membranes. Indeed, a similar qualitative transferability between membrane compositions has been observed previously regarding effects of peptide hydrophobicity (15, 19,20), length (16,17), charge (17), and topology (17). Having said that, we note that membrane defect formation is merely one aspect of the antimicrobial action of AMPs (5), hence no further claim is made on the biological relevance of the presently obtained data on POPC-d_{31} to bacterial or other systems.

In order to learn more on the underlying reasons behind the increased liposome rupture for the hydrophobically modified CNY21L and CNY21WWW peptides, ellipsometry studies were performed to determine the amount of peptide bound to the lipid membrane. As can be seen in Figure 2a for POPC-d_{31} in the absence of cholesterol, H->L and WWW-tagging both promote peptide adsorption, particularly so for the WWW-tagging. As with liposome leakage, these results are quite similar to those previously obtained for DOPC and DOPE/DOPG bilayers (15,18,19), as is the minute adsorption of the WWW tripeptide. For cholesterol-supplemented POPC-d_{31} bilayers, a similarly much higher adsorption was observed for the end-tagged CNY21WWW peptide (Figure 2b), while the WWW tripeptide again displayed only minute adsorption, expected from the high entropy loss per amino acid on adsorption, typically observed for low molecular polymers in general (43). Interestingly, the difference in adsorption between CNY21 and CNY21L was quite modest in the presence of cholesterol, in agreement with previous findings for DOPC/cholesterol (15).

In order to learn more on the localization of the peptides in the lipid membranes, tryptophan fluorescence spectra were monitored for CNY21WWW and the WWW tripeptide. As can be seen in Figure 3, the WWW tripeptide displayed identical W fluorescence spectra in buffer solution and in the presence of liposomes. This is expected from the very low WWW tripeptide adsorption at POPC-d_{31} and POPC-d_{31}/cholesterol membranes discussed above. For CNY21WWW, a minor decrease in fluorescence intensity was observed in the presence of liposomes, comparable for POPC-d_{31} and POPC-d_{31}/cholesterol liposomes, an effect of a slightly lower polarity in the immediate vicinity of the W residues when the peptide is bound

to the lipsome (42). Furthermore, CNY21WWW displayed no blueshift of the position of the fluorescence peak, indicating that its W groups are in a highly polar environment (42), i.e., localized in the polar headgroup region of the phospholipid membranes. Similar results were obtained also with anionic POPE/POPG liposomes (Supporting material, Figure 3). Furthermore, CD showed limited secondary structure induction in the presence of liposomes (Figure 4). Quantitatively, the CD spectra indicate the random coil to be the dominating conformation, with some helix content as well (10/11/11% and 20/21/20% for CNY21 and CNY21L, respectively in buffer, POPC, and POPC/cholesterol, respectively). For CNY21WWW, quantification of the helix content is more complicated due to contributions to the CD signal from the W side chains, however by comparing spectra for CNY21, CNY21WWW, and WWW, one can conclude that the helix content of CNY21WWW is certainly less than 15%. Together, fluorescence spectroscopy and CD data exclude ordered transmembrane structures. Since previous electrochemistry findings (18) have shown that CNY21 binds among or ontop the polar headgroups in the case of structurally similar DOPC, the combined data suggest a surface localization for the entire CNY21WWW peptide.

To learn more about the effects of peptide hydrophobization on membrane localization and structure, however, a more precise method than W fluorescence and CD spectroscopy is needed. The next step in our investigation was therefore to monitor lipid structure and dynamics with solid state NMR for macroscopically oriented bilayers. As described in the Experimental section, macroscopically oriented POPC-d_{31} bilayers gave rise to a series of deuterium splittings in the NMR spectra, from which the order parameter of the corresponding methylene group could be deduced (increased splitting corresponding to increased ordering). Figure 5 shows NMR deuterium spectra for oriented samples without (a) and with (b) 40 mol% cholesterol. The presence of cholesterol increased the magnitude of these splittings, a consequence of the condensing effect of cholesterol (36,43). This condensation leads to an increase in the ordering of the lipid molecules in relation to the bilayer normal and consequently also to an increase in the observed splittings (44). In quantitative terms, the maximum order parameter was found to increase from 0.19 to 0.34 for the peptide-free bilayers, in agreement with previous findings on POPC-d_{31} as well as related systems (27,45,46). As expected, given the minute binding of the WWW tripeptide to POPC-d_{31} bilayers (Figure 2), this peptide had only marginal effects on the lipid ordering. Both CNY21L and CNY21WWW, on the other hand, disordered the lipid acyl chains. This peptide-induced disordering is compatible with peptide adsorption causing lateral expansion

of the lipid membrane, in turn resulting in acyl group stretching relaxation (47,48). The peptide disordering effect is observable for all resolved peaks in Figure 5a, i.e., in all methylene groups within the POPC-d_{31} palmitoyl chain. Interestingly, bilayers of POPC-d_{31} and POPC-d_{31}/cholesterol behaved somewhat differently in terms of the relative importance of the CNY and the WWW moieties for lipid chain disordering. In Figure 6, the relative change in ordering is plotted for the resolved peaks in Figure 5, starting from the center (least ordered) peak. If the assumption is made that the ordering of the methylene segments is monotonically increasing from the C_{16} segment and upwards in the chain, the first position would correspond to the terminal methyl group and the following positions correspond to methylene groups successively higher up in the chain. The last position (most ordered) corresponds to overlapping signals from methylene groups in the plateau of the order parameter profile, i.e., approximately carbon numbers 3-8. As shown in Figure 6, CNY21L was found to be more potently disordering than CNY21WWW for POPC-d_{31} in the absence of cholesterol, despite the larger degree of adsorption for CNY21WWW (Figure 2). The large disordering effect found for CNY21L is consistent with previous electrochemistry findings, demonstrating penetration of this peptide into DOPC membrane interior (18). The relatively smaller effect observed for CNY21WWW suggests that the WWW moiety is located in the (outer part) of the polar headgroup region, consistent with a number of previous studies on membrane partitioning for antimicrobial peptides, where aromatic and polarizable W (and F) residues have been found to have an affinity to interfaces, and to be located in the proximity of the polar headgroup region in phospholipid membranes (49-52). In the case of antimicrobial peptides, examples of this have been provided, e.g., by Glukhov et al., who found sequence-dependent penetration of KKKKKKAAXAAWAAXAA (X being W or F) of 2.5-8Å (49). Furthermore, Li et al., investigated aurein 1.2 analogs and found the F residues in these peptides to penetrate 2-5Å below the polar headgroup region (50). Through this interaction with the phospholipid membrane, W/F residues are able to insert into the membrane, acting as an anchor for the peptide (51).

In the presence of cholesterol, CNY21L caused substantially less lipid disordering than in its absence, and the lipid disordering effect decayed more quickly when moving towards the membrane interior (Figure 5b). Both these effects are most likely due to CNY21L being unable to penetrate into the inner parts of the lipid membrane in the presence of cholesterol, although still adsorbing at the outer part of the lipid membrane to a high extent (Figure 2). In contrast, CNY21WWW was able to disorder the lipid chains effectively, as well as to adsorb

extensively, also for the cholesterol-supplemented bilayers. The seemingly higher disordering caused by CNY21WWW in the presence of cholesterol is a reflection of the higher order in the cholesterol-containing membrane per se. Hence, what the results show is that CNY21WWW is able to insert into the interfacial region of the membrane, thereby reducing the lipid condensation caused by cholesterol. Thus, for POPC-d$_{31}$ the affinity of W to the membrane interface is strong enough to cause a reduction of the lipid packing induced by cholesterol.

The findings obtained from deuterium splittings and order parameters are supported also by data on lateral diffusion coefficients for the lipid in the absence and presence of the peptides. The lipid diffusion is goverened mainly by the available free area for diffusion jumps (53). It is also believed that the location of the peptide in the bilayer is important for determining the lateral diffusion due to the high lateral pressure exerted in this region. Thus, peptides being able to penetrate into the interfacial region will have a larger impact on lipid diffusion than peripherally bound peptides, due to larger obstruction for submerged peptides than for peptides sitting essentially ontop of the polar headgroups. As can be seen in Figure 7, the WWW tripeptide had only marginal effect on the lipid diffusion, expected given the very limited adsorption of this peptide to the lipid membranes. In the absence of cholesterol, both CNY21L and CNY21WWW caused substantial reduction in the lipid self-diffusion. Given the much higher adsorption of CNY21WWW, similar membrane location would yield an excluded area for this peptide ≈6 times larger than that of CNY21L. That relative comparable reductions in the lipid diffusion coefficient are observed for the two peptides, despite this difference in adsorption, suggest a deeper penetration of CNY21L in the cholesterol-void POPC-d$_{31}$ bilayers, consistent with the findings discussed above. Again in agreement with the quadropolar splittings results discussed above, cholesterol ordered the lipid membrane, and resulted in a well-established reduction of the lipid lateral diffusion (27,53). Furthermore, CNY21L caused a substantially lower reduction in D$_{L}$ in the presence than in the absence of cholesterol, consistent with a less pronounced penetration of this peptide to the membrane interior in the presence of cholesterol. CNY21WWW, on the other hand, was able not only to adsorb extensively to cholesterol-supplemented POPC-d$_{31}$ bilayers, but also achieve an (albeit minor) penetration, and to substantially reduce D$_{L}$, primarily through excluded area effects (Figure 8).

The present findings are in accordance to those previously reported on studies using a comparable NMR methodology for amphiphilic peptides. For example, MSI-78 and MSI-594, extensively investigated peptides derived from magainin-2 and melittin (54,55), as well as ampullosporin A (56), have all been found to localize in (the vicinity of) the polar headgroup region of the phospholipid membranes, and with an orientation parallel to the membrane surface. Also ^{2}H solid state NMR on oriented bilayers has been applied to investigating such systems. For example, Aisenbrey et al. used this approach, together with use of peptides labelled with 3,3,3-^{2}H$_3$-alanines, in order to probe orientation of polypeptide bonds normal to the bilayer normal (57). More directly related to the present work, ^{2}H NMR has previously been used also for probing membrane order and pertubation, e.g., for POPC and POPE/POPG bilayers in the presence and absence of cholesterol, and in the presence of antimicrobial peptides (58). In agreement with the finding of the present investigation, the latter study reports on a strongly ordering effect of cholesterol, as well as on a strongly disordering effect on membrane fatty acyl chains by peptides residing in the surface region of the phospholipid membrane.

Conclusions

Increasing peptide hydrophobicity of the complement-derived antimicrobial peptide CNY21 through either H->L substitutions or end-tagging with WWW promotes peptide adsorption to both anionic and zwitterionic phospholipid membranes, as well as membrane rupture in both the corresponding liposomes and bacteria. The way of hydrophobizing the peptide affects the magnitude of these effects, as well as peptide incorporation to the interior of phospholipid membranes and peptide susceptibility to presence of cholesterol in the phospholipid membrane, the latter demonstrated through the use of NMR techniques for macroscopically oriented phospholipid bilayers. Given that comparable results on a higher membrane-lytic efficiency for the CNY21L and CNY21WWW were found for bacteria and model lipid liposomes (also obviously "non-biological" ones as POPC-d$_{31}$), even results from seemingly less relevant model systems may have at least some bearing on the mechanism of bacteria membrane disruption for this type of antimicrobial peptides. Having said that, it must be understood that biological effects depend substantially on cell type and bacteria strain, and that both peptide binding and resulting membrane disruption depend strongly on a range of factors, such as local pH, electrolyte concentration, presence of AMP scavangers (e.g.,

glucose aminoglycans, bacterial lipopolysaccharides, and extracellular polysaccharides) released from bacteria, and presence and concentration of both bacterial and cell proteases. Studies with model lipid membranes therefore need to be paralleled by investigations in the biological systems.

Acknowledgement

Supporting material

Results on peptide-induced POPE/POPG (75/25) liposome leakage, peptide-induced killing of *E. coli and P. aeruginosa* obtained by viable count analysis, as well as tryptophan fluorescence spectra for CNY21WWW and WWW in the presence of POPE/POPG (75/25) liposomes are available as supporting materials.

References

1. French, G.L. (2005) Clinical impact and relevance of antibiotic resistance. *Adv. Drug Deliv. Rev.* **57**, 1514-1527.

2. Zasloff, M. (2002) Antimicrobial peptides of multicellular organisms. *Nature* **415**, 389-395.

3. Marr, A.K., Gooderham, W.J., and Hancock, R.E. (2006) Antibacterial peptides for therapeutic use: obstacles and realistic outlook. *Curr. Opin. Pharmacol.* **6**, 468-472.

4. Tossi, A., Sandri, L., and Giangaspero, A. (2000) Amphipathic, alpha-helical antimicrobial peptides. *Biopolymers* **55**, 4-30.

5. Brogden, K.A. (2005) Antimicrobial peptides: pore formers or metabolic inhibitors in bacteria? *Nat. Rev. Microbiol.* **3**, 238-250.

6. Nizet, V. (2006) Antimicrobial peptide resistance mechanisms of human bacterial pathogens. *Curr. Issues Mol. Biol.* **8**, 11-26.

7. Huang, H.W. (2006) Molecular mechanism of antimicrobial peptides: the origin of cooperativity. *Biochim. Biophys. Acta* **1758**, 1292-1302.

8. Hancock, R.E. and Sahl, H.G. (2006) Antimicrobial and host-defense peptides as new anti-infective therapeutic strategies. *Nat. Biotechnol.* **24**, 1551-1557.

9. Zelezetsky, I. and Tossi, A. (2006) Alpha-helical antimicrobial peptides-using a sequence template to guide structure-activity relationship studies. *Biochim. Biophys. Acta* **1758**, 1436-1449.

10. Bhonsle, J.B., Venugopal, D., Huddler, D.P., Magill, A.J., and Hicks, R.P. (2007) Application of 3D-QSAR for identification of descriptors defining bioactivity of antimicrobial peptides. *J. Med. Chem.* **50**, 6545-6553.

11. Pasupuleti, M., Walse, B., Svensson, B., Malmsten, M., and Schmidtchen, A. (2008) Rational design of antimicrobial C3a analogues with enhanced effects against Staphylococci using an integrated structure and function-based approach. *Biochemistry* **47**, 9057-9070.

12. Anderson Nordahl, E., Rydengård, V., Nyberg, P., Nitsche, D.P., Mörgelin, M., Malmsten, M., Björck, L., and Schmidtchen, A. (2004) Activation of the complement system generates antibacterial peptides. *Proc. Natl. Acad. Sci. U S A* **101**, 16879-16884.

13. Malmsten, M., Davoudi, M., and Schmidtchen, A. (2006) Bacterial killing by heparin-binding peptides from PRELP and thrombospondin. *Matrix Biol.* **25**, 294-300.

14. Malmsten, M., Davoudi, M., Walse, B., Rydengård, V., Pasupuleti, M., Mörgelin, M., and Schmidtchen, A. (2007) Antimicrobial peptides derived from growth factors. *Growth Factors* **25**, 60-70.

15. Ringstad, L., Andersson Nordahl, E., Schmidtchen, A., and Malmsten, M. (2007) Composition effect on peptide interaction with lipids and bacteria: variants of C3a peptide CNY21. *Biophys. J.* **92**, 87-98.

16. Ringstad, L., Schmidtchen, A., and Malmsten, M. (2006) Effect of peptide length on the interaction between consensus peptides and DOPC/DOPA bilayers. (2006) *Langmuir* **22**, 5042-5050.

17. Ringstad, L., Kacprzyk, L., Schmidtchen, A., and Malmsten, M. (2007) Effects of topology, length, and charge on the activity of a kininogen-derived peptide on lipid membranes and bacteria. *Biochim. Biophys. Acta* **1768**, 715-727.

18. Ringstad, L., Protopapa, E., Lindholm-Sethson, B., Schmidtchen, A., Nelson, A., and Malmsten, M. (2008) An electrochemical study into the interaction between complement-derived peptides and DOPC mono- and bilayers. *Langmuir* **24**, 208-216.

19. Schmidtchen, A., Pasipuleti, M., Mörgelin, M., Davoudi, M., Alenfall, J., Chalupka, A. and Malmsten, M. (2009) Boosting antimicrobial peptides by hydrophobic amino acid end-tags. *J. Biol. Chem.* **284**, 17584-17594.

20. Pasupuleti, M., Schmidtchen, A., Chalupka, A., Ringstad, L., and Malmsten, M. (2009) End-tagging of ultra-short antimicrobial peptides by W/F stretches to facilitate bacterial killing. *PLoS One* **4**, 1-9.

21. Pasupuleti, M., Chalupka, A., Mörgelin, M., Schmidtchen, A., and Malmsten, M. (2009) Tryptophan end-tagging of antimicrobial peptides for increased potency against *Pseudomonas aeruginosa*. *Biochim. Biophys. Acta* **1790**, 800-808.

22. Strömstedt, A.A., Pasupuleti, M., Schmidtchen, A., and Malmsten, M. (2009) Oligotryptophan-tagged antimicrobial peptides and the role of the cationic sequence. *Biochim. Biophys. Acta* **1788**, 1916-1923.

23. Malmsten, M. (1994) Ellipsometry studies of protein layers adsorbed at hydrophobic surfaces. *J Colloid Interface Sci* **166**, 333-342.

24. Tiberg, F., Harwigsson, I., and Malmsten, M. (2000) Formation of model lipid bilayers at the silica-water interface by co-adsorption with non-ionic dodecyl maltoside surfactant. *Eur. Biophys. J.* **29**, 196-203.

25. De Feijter, J.A., Benjamins, J., and Veer, F.A. (1978) Ellipsometry as a tool to study the adsorption behavior of synthetic and biopolymers at the air-water interface. *Biopolymers* **17**, 1759-1772 .

26. Malmsten, M., Burns, N., and Veide, A. (1998) Electrostatic and hydrophobic effects of oligopeptide insertions on protein adsorption. *J. Colloid Interface Sci.* **204**, 104-111.

27. Lindblom, G. and Orädd, G. (2009) Lipid lateral diffusion and membrane heterogeneity. *Biochim. Biophys. Acta.* **1788**, 234-244.

28. Filippov, A., Orädd, G., and Lindblom, G. (2003) Influence of cholesterol and water content on phospholipid lateral diffusion in bilayers. *Langmuir* **19**, 6397-6400.

29. Raleigh, D.P., Olejnicak, E.T., and Griffin, R.G. (1989) Broadband pulses for excitation and inversion in I=1 systems. *J. Magn. Res.* **81**, 455-463.

30. Burnett, L.J. and Muller, B.H., (1971) Deutron quadrupole coupling constants in three solid deuterated paraffin hydrocarbons: $C_2D_6C_4D_{10}$, C_6D_{14}. *J. Chem. Phys*. **55**, 5829-5831.

31. Davis, J.H. (1983) The description of membrane lipid conformation, order and dynamics by ^{2}H-NMR. *Biochim. Biophys. Acta* **737**, 117-171.

32. Orädd, G. and Lindblom, G. (2007) Lateral diffusion coefficients of raft lipids from pulsed field gradient NMR. *Methods in Molecular Biology* (Clifton, USA) **398**, 127-142.

33. Tanner, J.E. (1970) Use of the stimulated echo in NMR diffusion studies. *J.Chem.Phys.* **52**, 2523-2526.

34. Gibbs, S.J. and Johnson, C.S. Jr. (1991) A pfg NMR experiment for accurate diffusion and flow studies in the presence of eddy currents. *J. Magn. Res.* **93**, 395-402.

35. Stilbs, P., Paulsen, K., and Griffiths, P.C. (1996) Global least-squares analysis of large, correlated spectral data sets: application to component-resolved FT-PGSE NMR spectroscopy. *J. Phys. Chem.* **100**, 8180 - 8189.

36. Mouritsen, O.G. and Zuckermann, M.J. (2004) What's so special about cholesterol? *Lipids* **39**, 1101-1113.

37. Yeagle, P.L. (1993) The membranes of cells. Academic Press, San Diego.

38. Zwaal, R.F.A. and Schroit, A.J. (1997) Patophysiologic implications of membrane phospholipid assymetry in blood cells. *Blood* **89**, 1121-1132.

39. Rothman, J.E. and Lenard, J. (1977) Membrane asymmetry. *Science* **195**, 743-753.

40. Bretscher, M.S. (1972) Assymetrical lipid bilayer structure for biological membranes. *Nature* **236**, 11-12.

41. Fleer, G.J., Cohen Stuart, M.A., Scheutjens, J.M.H.M., Cosgrove, T., and Vincent, B. (1993) Polymers at interfaces. Chapman & Hall, London.

42. Lotte, K., Plessow, R., and Brockhinke, A. (2004) Static and time-resolved fluorescence investigations of tryptophan analogues--a solvent study. *Photochem. Photobiol. Sci.* **3**, 348-359.

43. Leathes, J.B. (1925) Role of fats in vital phenomena. *Lancet* **208**, 853-856.

44. Vist, M.R. and Davis, J.H. (1990) Phase equilibria of cholesterol/dipalmitoylphosphatidylcholine mixtures: 2H nuclear magnetic resonance and differential scanning calorimetry, *Biochemistry* **29**, 451-856.

45. Huster, D., Scheidt, H.A., Arnold, K., Herrmann, A., and Müller, P. (2005) Desmosterol may replace cholesterol in lipid membranes. *Biophys. J.* **88**, 1838-1844.

46. Henriksen, J., Rowat, A.C., Brief, E., Hsueh, Y.W., Thewalt, J.L., Zuckermann, M.J., and Ipsen, J.H. (2006) Universal behavior of membranes with sterols. *Biophys. J.* **90**, 1639-1649.

47. Heller, W.T., Waring, A.J., Lehrer, R.I., Harroun, T.A., Weiss, T.M., Yang, L., and Huang, H.W. (2000) Membrane thinning effect of the β-sheet antimicrobial protegrin. *Biochemistry* **39**, 139 -145.

48. Ludtke, S., He, K., and Huang, H. (1995) Membrane thinning caused by magainin 2. *Biochemistry* **34**,16764-16769.

49. Glukhov, E., Stark, M., Burrows, L.L., and Deber, C.M. (2005) Basis for selectivity of cationic antimicrobial peptides for bacterial versus mammalian membranes. *J. Biol. Chem.* **280**, 33960-33967.

50. Li, X., Li, Y., Peterkofsky, A., and Wang, G. (2006) NMR studies of aurein 1.2 analogs. *Biochim. Biophys. Acta* **1758**, 1203-1214.

51. Deslouches, B., Phadke, S.M., Lazarevic, V., Cascio, M., Islam, K., Montelaro, R.C., and Mietzner, T.A. (2005) De novo generation of cationic antimicrobial peptides: influence of length and tryptophan substitution on antimicrobial activity. *Antimicrob. Agents Chemother.* **49**, 316-322.

52. McInturff, J.E., Wang, S.-J., Macleidt, T., Lin, T.R., Oren, A., Hertz, C.J., Krutzik, S.R., Hart, S., Zeh, K., Anderson, D.H., Gallo, R.L., Modlin, R.L., and Kim, J. (2005) Granulysin-derived peptides demonstrate antimicrobial and anti-inflammatory effects against *Propionibacterium acnes*. *J. Invest. Dermatol.* **125**, 256-263.

53. Almeida, P.F.F., Vaz, W.L.C., and Thompson, T.E. (1992) Lateral diffusion in the liquid phases of dimyristoylphosphatidylcholine cholesterol lipid bilayers – a free-volume analysis. *Biochemistry* **31**, 6739-6747.

54. Glotter, L.M. and Ramamoorthy, A. (2009) Structure, membrane orientation, mechanism, and function of pexiganal – a highly potent antimicrobial peptide designed from magainin. *Biochim. Biophys. Acta* **1788**, 1680-1686.

55. Ramamoorthy, A., Thennarasu, S., Lee, D.K., Tan, A., and Maloy, L. (2006) Solid-state NMR investigation of the membrane-disrupting mechanism of antimicrobial peptides MSI-78 and MSI-594 derived from magainin 2 and melittin. *Biophys. J.* **91**, 206-216.

56. Salnikov, E.S., Friedrich, H., Li, X., Bertani, P., Reissmann, S., Hertweck, C., O'Neil, J.D.J., Raap, J., and Bechinger, B. (2009) Structure and alignment of the membrane-associated ampullosporin A and alamethicin by oriented ^{15}N and ^{31}P solid-state NMR spectroscopy. *Biophys. J.* **96**, 86-100.

57. Aisenbrey, C., Bertani, P., Henklein, P., and Bechinger, B. (2007) Structure, dynamics and topology of membrane peptides by oriented ^{2}H solid-state NMR spectroscopy. *Eur. Biophys. J.* **36**, 451-460.

58. Salnikov, E.S., Mason, A.J., and Bechinger, B. (2009) Membrane order pertubation in the presence of antimicrobial peptides by ^{2}H solid-state NMR spectroscopy. *Biochimie* **91**, 734-743.

59. Eisenberg, D., Schwarz, E., Komaromy, M., and Wall, R. (1984) Analysis of membrane and surface protein sequences with the hydrophobic moment plot. *J. Mol. Biol.* **179**, 125-142.

Table 1. Primary structure and key properties of the peptides investigated.

CNYITELRRQHARASHLGLAR   (CNY21)

CNYITELRRQ**L**ARAS**L**LGLAR   (CNY21L)

CNYITELRRQHARASHLGLAR**WWW**   (CNY21WWW)

WWW   (WWW)

	CNY21	*CNY21L*	*CNY21WWW*
IP^1	10.7	10.7	10.7
Z_{net}^2 *(pH 7.4)*	+3	+3	+3
H^3	-0.33	-0.24	-0.24

[1] IP:isoelectric point; [2]Z_{net}: net charge; ^{3}H mean hydrophobicity on the Eisenberg scale (59).

Figure Captions

Figure 1 Peptide-induced liposome leakage for POPC-d_{31} (a) and POPC-d_{31}/cholesterol (60/40 mol/mol) (b) in 10 mM Tris, pH 7.4.

Figure 2 Peptide adsorption to POPC-d_{31} (a) and POPC-d_{31}/cholesterol (60/40 mol/mol) (b) bilayers in 10 mM Tris, pH 7.4.

Figure 3 Tryptophan fluorescence spectra, at a peptide concentration of 10 μM, for CNY21WWW (a) and tripeptide WWW (b) in 10 mM Tris, pH 7.4, with or without POPC-d_{31} or POPC-d_{31}/cholesterol (60/40 mol/mol) liposomes (100 μM lipid).

Figure 4 CD spectra for CNY21 (a), CNY21L (b), CNY21WWW (c), and WWW (d) in 10 mM Tris, pH 7.4, with or without POPC-d_{31} or POPC-d_{31}/cholesterol (60/40 mol/mol) liposomes (100 μM lipid).

Figure 5 NMR deuterium spectra from macroscopically oriented bilayers of POPC-d_{31} without (a) or with (b) cholesterol (40 mol%) in Tris buffer, pH 7.4.

Figure 6 Peptide-induced change in quadrupole splitting (Δv_q) for individual peaks of POPC-d_{31} in macroscopically oriented bilayers of POPC-d_{31} without (a) or with (b) cholesterol (40 mol%) in Tris buffer, pH 7.4.

Figure 7 (a) Peptide-induced changes in the two-dimensional diffusion coefficient (D_L) of POPC-d_{31} in macroscopically oriented bilayers of POPC-d_{31} with or without cholesterol (40 mol%) in Tris buffer, pH 7.4.

Figure 8 Schematic illustration of membrane localization of CNY21L and CNY21WWW in POPC membranes. In the absence of cholesterol, CNY21L penetrates into the aliphatic membrane interior, while in the presence of cholesterol, the peptide is unable to do so. CNY21WWW displays relatively shallow localization in the membrane irrespective of cholesterol, but is not excluded from the membrane by cholesterol. Instead, through causing substantial area expansion, it disorders POPC membranes both in the absence and presence of

cholesterol. In comparison to these peptides, CNY21 has previously been shown to be localized in the headgroup region (18).
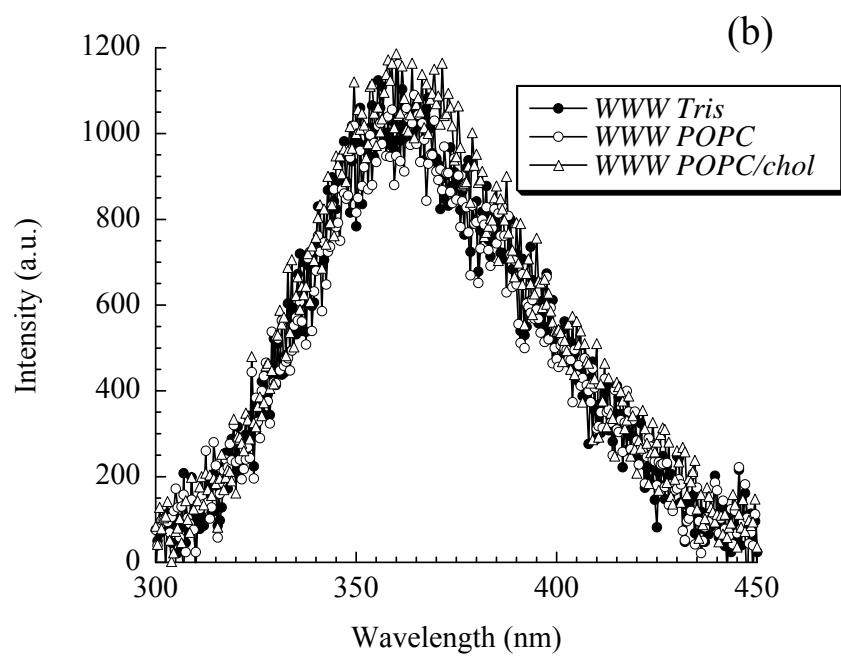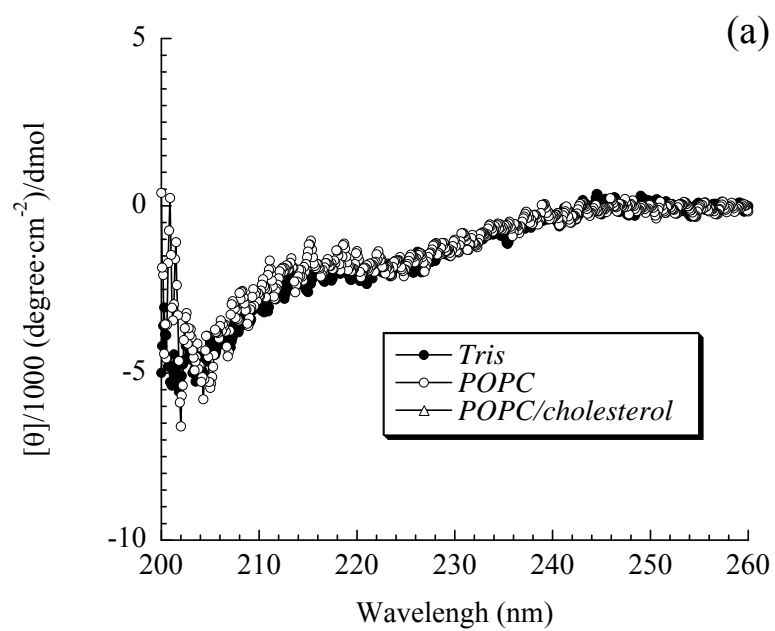
Figure 1.
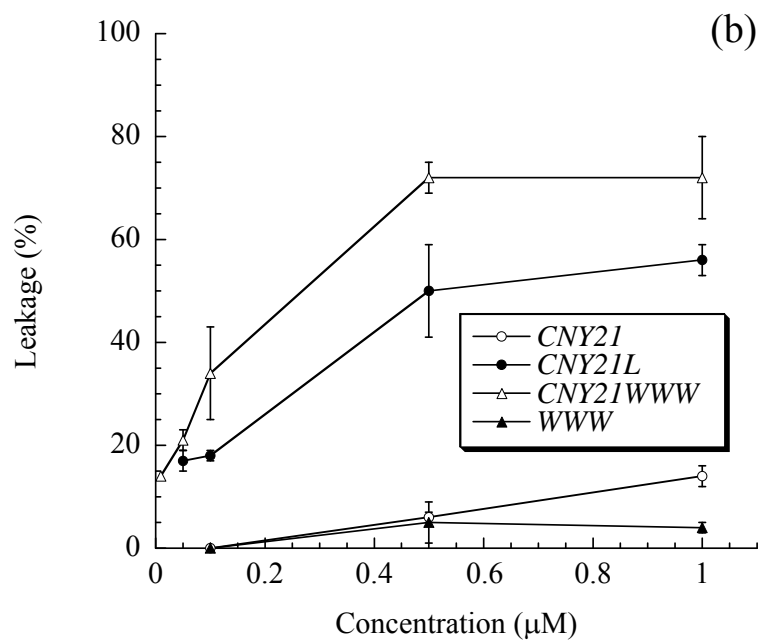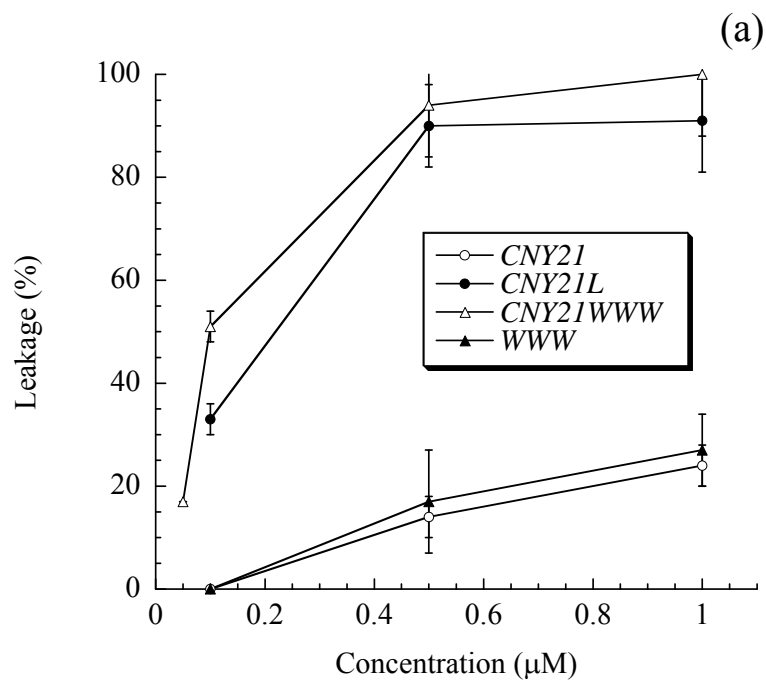
Figure 2.

Figure 3.

Figure 4.

(c)

(d)

Figure 5.

(a)

+WWW

+CNY21WWW

+CNY21L
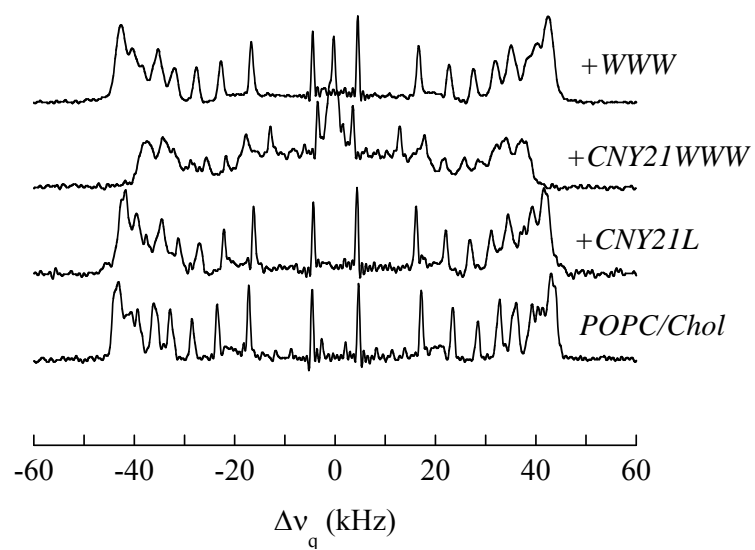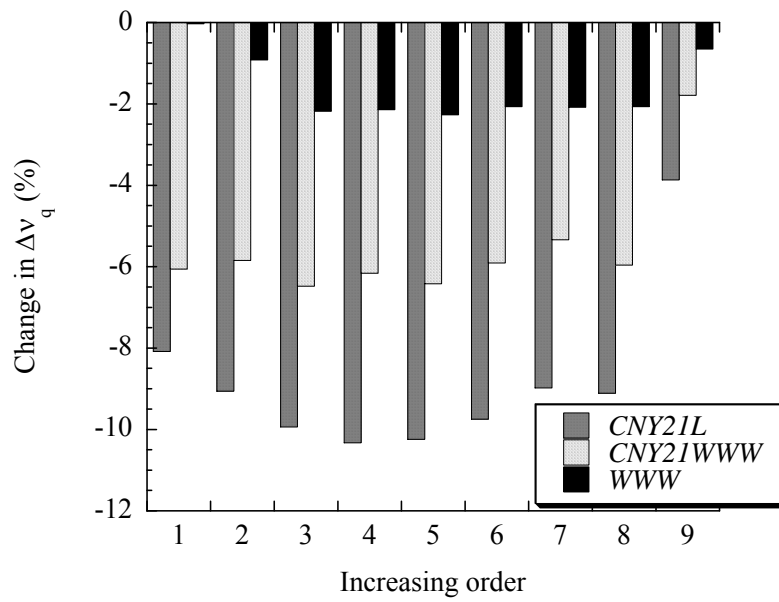
POPC

$\Delta\nu_q$ (kHz)

(b)

+WWW

+CNY21WWW

+CNY21L

POPC/Chol

$\Delta\nu_q$ (kHz)
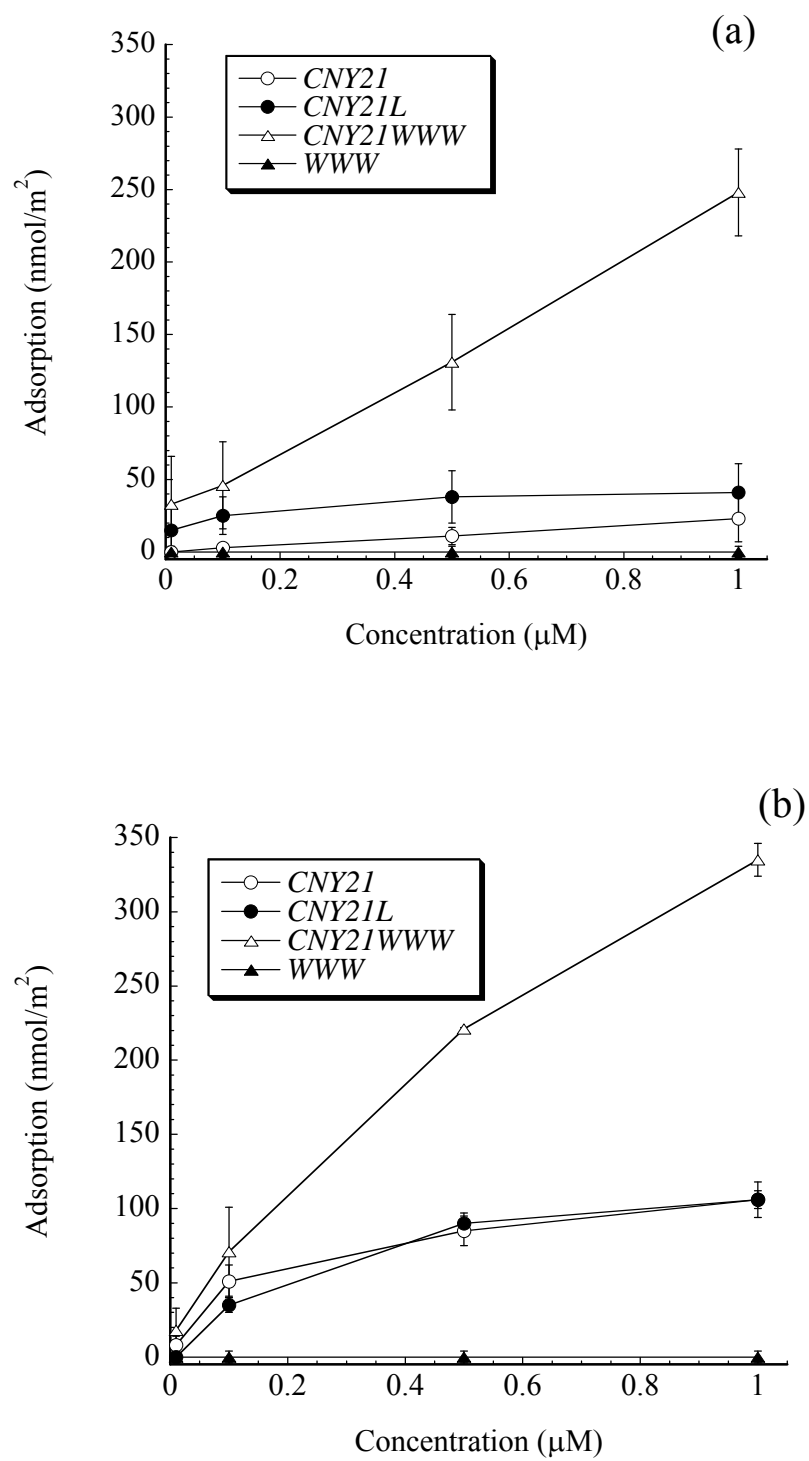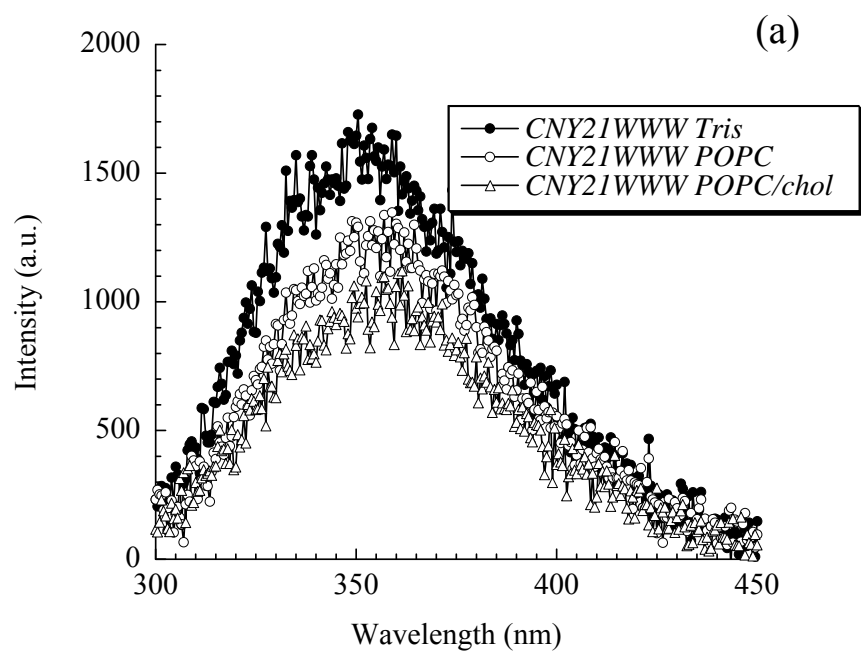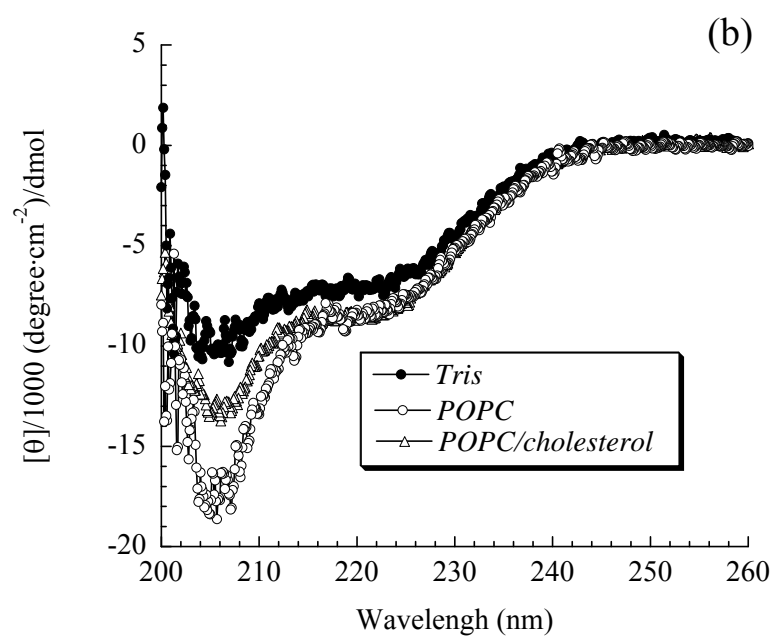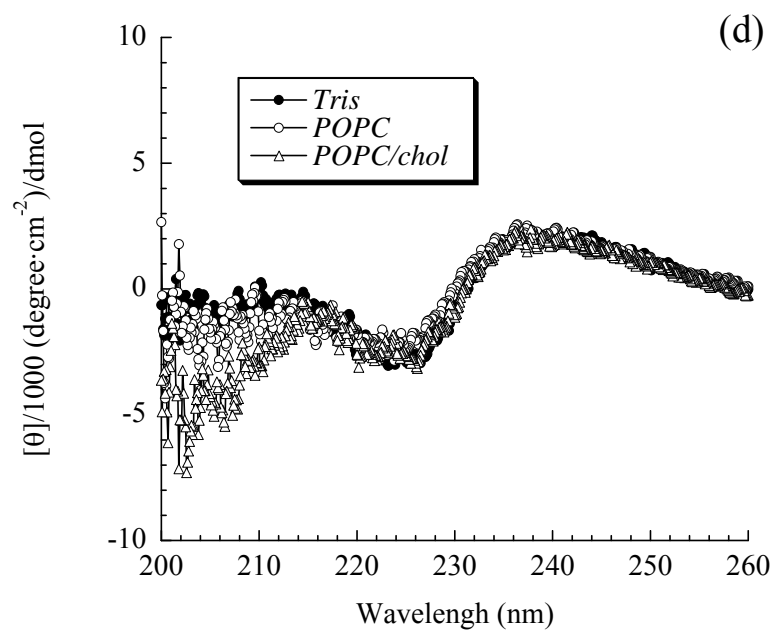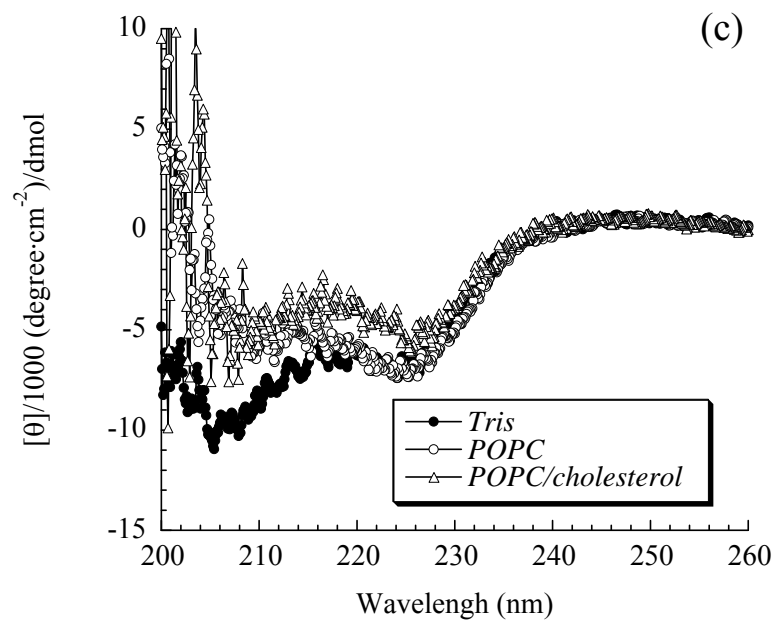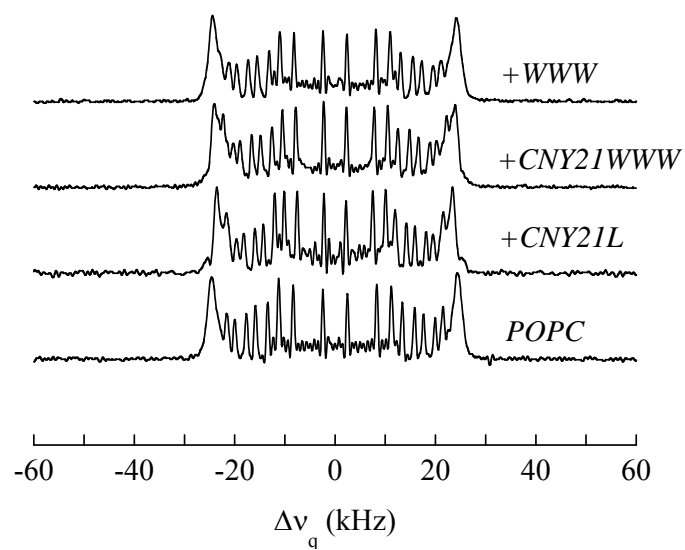
Figure 6.

(a)

(b)

Figure 7.

Figure 8.

CNY21L

Headgroup region

Carbonyl region

Aliphatic region

CNY21WWW

Headgroup region

Carbonyl region

Aliphatic region
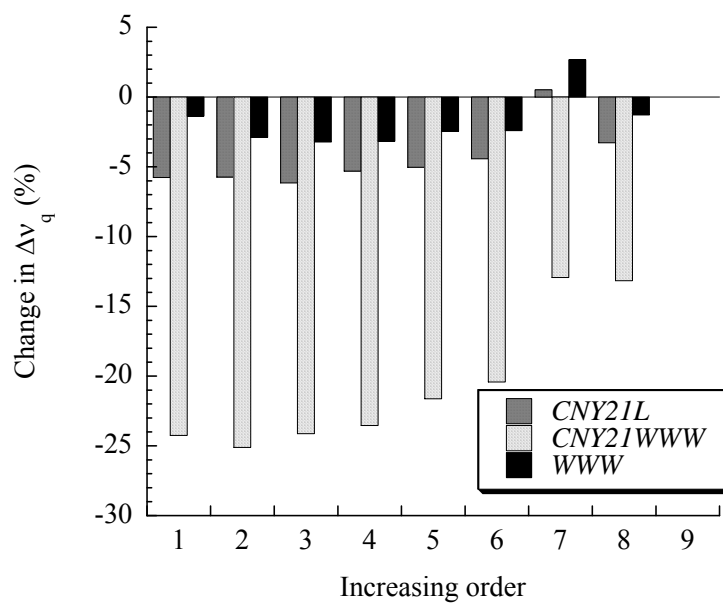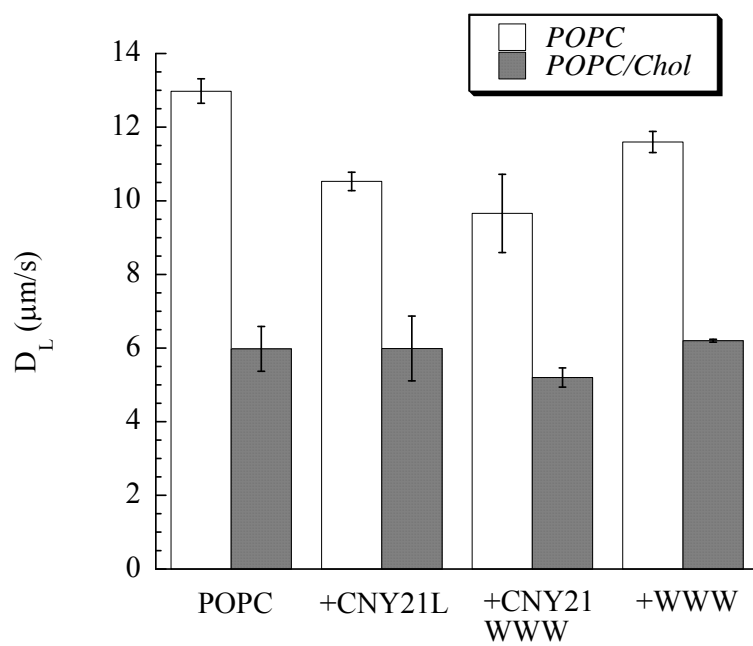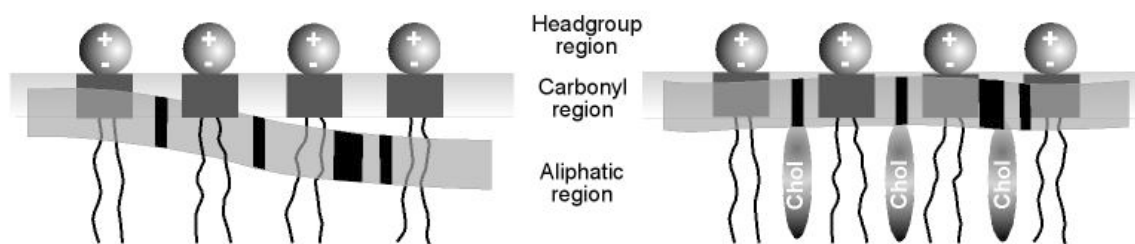
CNY21L

CNY21WWW
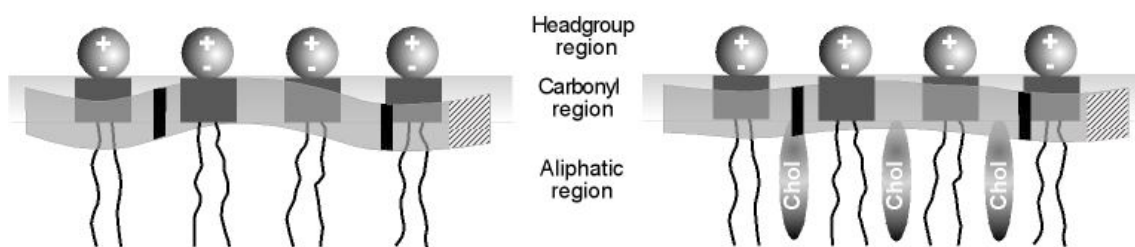
Supporting Material

Figure S1 Peptide-induced liposome leakage for POPE/POPG (75/25) in 10 mM Tris, pH 7.4.
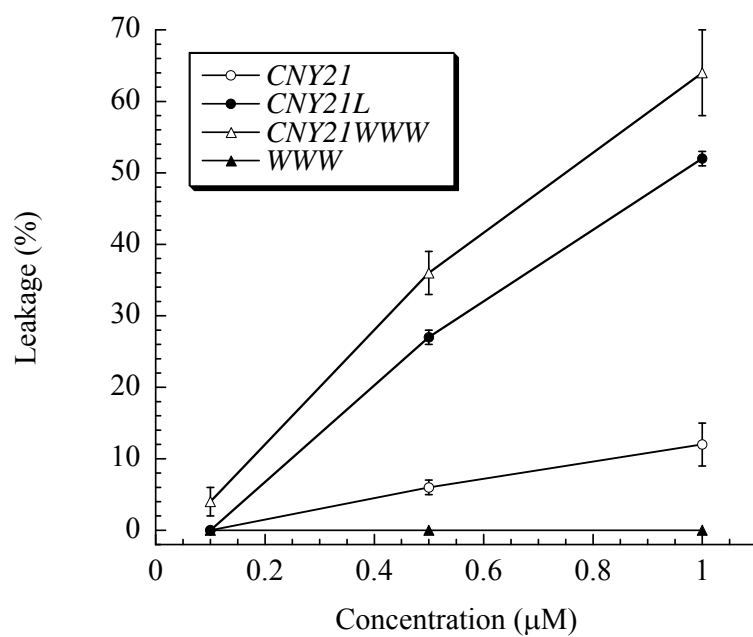
Figure S2 Viable count assay data on bactericidal effect of the peptides investigated against *E. coli* and *P. aeruginosa* at a concentration of 30 µM in 10 mM Tris, pH 7.4, with additional 150 mM NaCl.
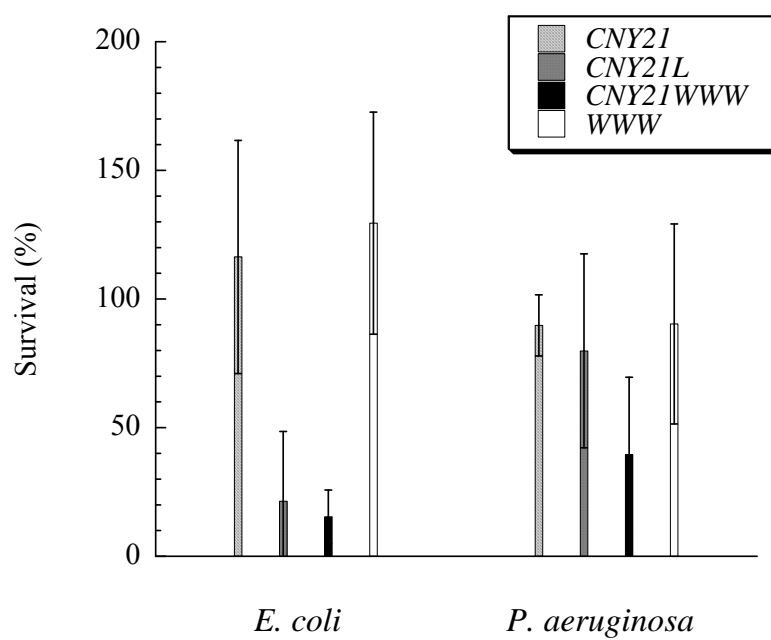
Figure S3 Tryptophan fluorescence spectra, at a peptide concentration of 10 μM, for CNY21WWW (a) and tripeptide WWW (b) in 10 mM Tris, pH 7.4, with or without POPE/POPG (PEPG; 75/25 mol/mol) liposomes (100 μM lipid).